An off-axis Four-Quadrant Phase-Mask coronagraph for Palomar: high contrast near bright stars imager

Pierre Haguenauer[a], Eugene Serabyn[a], Eric E. Bloemhof[a], James K. Wallace[a],
Robert O. Gappinger[a], Bertrand Mennesson[a], Mitchell Troy[a], Chris D. Koresko[a],
and James D. Moore[a]

[a]Jet Propulsion Laboratory, California Institute of Technology, 4800 Oak Grove Drive,
Pasadena, CA 91109, USA;

ABSTRACT

Direct detection of planets around nearby stars requires the development of high-contrast imaging techniques, because of their very different respective fluxes. This led us to investigate the new coronagraphic approach based on the use of a four-quadrant phase mask (FQPM). Combined with high-level wavefront correction on an unobscured off-axis section of a large telescope, this method allows high-contrast imaging very close to stars. Calculations indicate that for a given ground-based on-axis telescope, use of such an off-axis coronagraph provides a near-neighbor detection capability superior to that of a traditional coronagraph utilizing the full telescope aperture. A near-infrared laboratory experiment was first used to test our FQPM devices, and a rejection of 2000:1 was achieved. We next built an FQPM instrument to test the feasibility of near-neighbor observations with our new off-axis approach on a ground-based telescope. In June 2005, we deployed our instrument to the Palomar 200-inch telescope, using existing facilities as much as possible for rapid implementation. In these initial observations, stars were rejected to about the 100:1 level. Here we discuss our laboratory and on-sky experiments, and the results obtained so far.

Keywords: Coronagraphy, phase mask, Terrestrial Planet Finder.

1. INTRODUCTION

The exciting scientific goal of direct exoplanet detection requires the development of new measurement techniques to meet the exacting contrast requirements. Imaging a faint companion close to a much brighter star requires being capable of observing with high contrast ratio (ratio of the flux of the bright parent star to the flux of the fainter companion) at small inner working distance (IWD). However, practical issues such as large IWDs limit coronagraphs based on classical Lyot[1] techniques (use of an opaque disk to block the on-axis light). Of course, diffracted and scattered light limit all coronagraphs to varying extents. Different novel approaches are thus being studied to overcome these limitations[2–10].

This led us to implement a novel high-contrast coronagraph to allow for detection in the immediate vicinity of bright stars. This coronagraphic method uses a Four-Quadrant Phase Mask[3,11–14] (FQPM) in place of the opaque disk in a classical coronagraph, in conjunction with an off-axis section of the telescope, in order to ensure high rejection (ratio of the flux of a bright star without the coronagraph in place to the remaining flux for the same star with the coronagraph in place). The advantages of this approach are the capability of detecting companions very close to the parent star, together with a geometrical design that is wavelength independent.
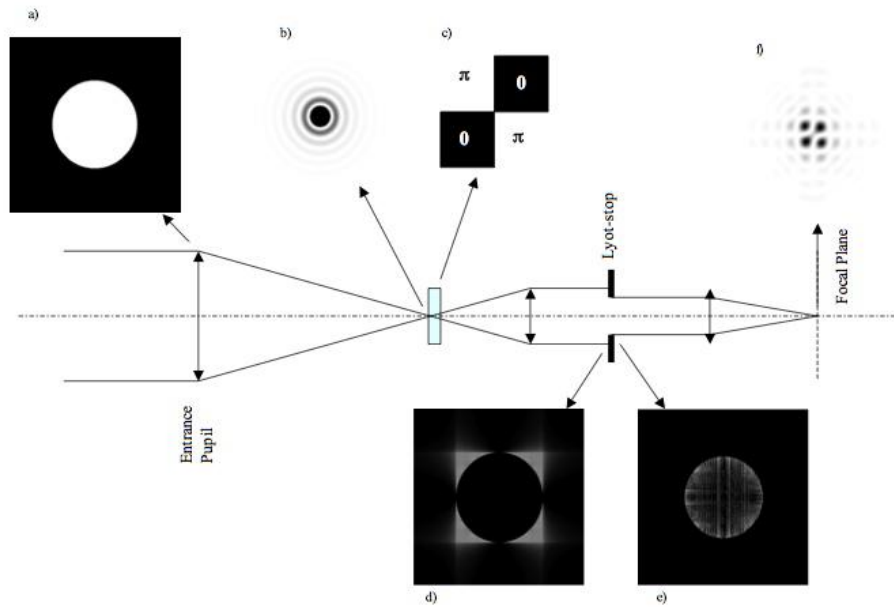
Figure 1. Principle of coronagraphy with a Four Quadrant Phase Mask.

2. FQPM PRINCIPLE

Figure 1 presents the principle of the coronagraph using a Four Quadrant Phase Mask[3]. The general setup is identical to the one of a classical Lyot coronagraph, but here the opaque occulting mask has been replaced by a transparent phase-mask providing a π phase shift in two diametrically opposed quadrants of the incoming focal-plane electric field. A circular unobscured pupil (a) gives an Airy disk (b) in the focal plane, which is focused at the exact crosshair of the mask (c). The mask is composed of four quadrants, the two of them diametrically opposed along one diagonal being phase-shifted by radians compared to the other two. Destructive interferences will then occur between the different part of the electric field, and in the next pupil plane (d), instead of a uniformly lighted circular disk, the flux is consequently repartitioned so that almost all the light is in the area surrounding the pupil, which is now visible as a dark disk. A Lyot stop (e) in this pupil plane, slightly smaller than the pupil size (90% here) then blocks the light surrounding the pupil (the intensity scales for images d and e are different for better clarity). When focusing the electric field obtained after the Lyot stop, one gets an image (f) where the flux in the center has been attenuated by a huge factor. Optimum attenuation occurs only for an object perfectly centered on the mask crosshair. Any off-axis object or structure in the nearby region of a star centered on the mask will thus not suffer this effect and remain visible. One advantage of such a phase mask is its symmetrical and achromatic design, compared to circular phase masks[2,9] where the size of the mask has to be adapted to each wavelength. This concept also allows measurements very close to the parent star (one Airy radius or lower), where classical amplitude masks have a dark region of several (3 to 10) Airy radius.
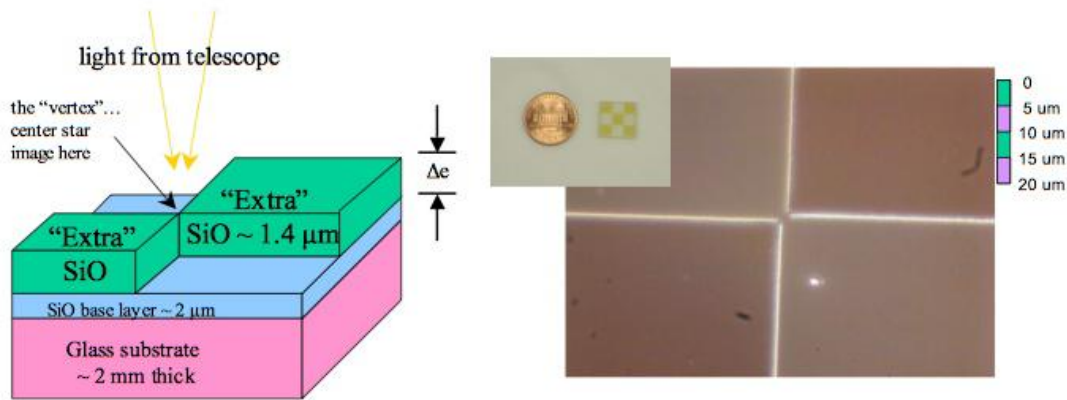
Figure 2. Realization of the FQPM: scheme of the deposited layers (left), and images of a fabricated FQPM (right).

3. MASK DESIGN

The Four Quadrant Phase Mask technique has been tested[13,14], but this promising solution for coronagraphy still requires technological development, manufacturing and experimental testing of these devices to obtain useful information and experience. When starting designing our devices some questions arise first:

- Should the design be first adapted to monochromatic or broadband operation?

- What precision is needed?

- Accordingly, what manufacturing technology is the most appropriate?

The choices we made are described in the following.

As we wanted to use existing facilities as much as possible for on-sky demonstration of the FQPM, the Palomar 200 inch telescope was chosen to take advantage of the facility adaptive optics system (see 5.1). Optimum rejection led also to the choice of the near-IR and especially the K-band atmospheric window for the operating wavelength. For broadband operation, the phase shift needs to be exactly π radians for all the wavelengths used. Such masks can be obtained by multilayer coatings[13] or newly proposed Zero Order Gratings[15]. Both of these techniques require sophisticated designs and fabrication processes. Trying these solutions first implied heavy work on the mask itself, which might not be compatible with fast on-sky testing and validation of the method. A single-layer deposition, i.e. a monochromatic mask, is a much easier process as it relies on existing lithography and layer deposition processes. The theoretical performance of such a mask[13] is a rejection factor of 45000:1 for a 1% bandwidth (e.g. in the Brackett gamma filter) and 240:1 for a 15% bandwidth (K short filter). As other factors, such as residual tip-tilt after the AO system, might limit the performance on ground telescopes to lower rejections, we made the choice of the more straightforward solution of depositing a single layer of dielectric on a glass substrate to create the phase shift.

The thickness of the layers providing the π phase shift in two quadrants is given by $\Delta e = (\lambda/2)/(n-1)$, with λ the operating wavelength and n the refractive index of the deposited material. For typical material used in deposition processes, this leads to Δe of the order of λ. The extent of the quadrants has to be many radii of the diffraction spot size in the focal plane to avoid compromising the rejection. For typical telescope parameters, the quadrants size has to be a few millimeters. We also wanted the edges of the quadrants to be sharp to a fraction of the Airy spot. The output of the Palomar Adaptive Optics System[16] (PALAO) is a f/16 beam, so at $\lambda = 2.2\mu m$, the spot FWHM is about $35\mu m$. With all the preceding taken into account, the following technology choices were made:

- Use standard photolithography which has a resolution of $1 - 2\mu m$,

- Thermal deposition of SiO which is easy to deposit and has an index of about 1.84 at $2.2\mu m$ (higher index means thinner layer to deposit),

- Choice of a high index glass to try to match as much as possible the SiO index and limit internal reflections inside the mask.

The mask fabrication design is presented in Fig. 2 (left). Our masks have been realized at the Micro-Devices Laboratory (MDL) at JPL. On a 2mm thick glass substrate, a SiO base layer is deposited over the entire bare substrate. This first layer allows balanced reflection coefficients between all the quadrants. An extra layer of SiO is then deposited on two of the quadrants using standard UV photolithographic masking techniques. Figure 2 right shows an example of a mask realized by this process. In the central panel, one can see one of our coin size masks, where the extra layer quadrants are visible (squares with a different color). Actually this device offers four vertices, i.e. four FQPM, where we can measure the extinction, thus allowing testing of the homogeneity of the deposition process. The second picture is a microscope image showing the crosshair between the quadrants. Microscope inspection of the mask allows checking the quality of the fabrication. The obtained film quality is high despite the fact that the deposited layer is rather thick, and the edges are straight. A vertex gap of about $2\mu m$ can be seen and the edges are out of place by about $1\mu m$, but modeling predicts that this is still compatible with a 1000:1 extinction goal. Electron-beam lithography, also available at the MDL facility, can deliver resolution in defined features that is several orders of magnitude finer than that achieved with optical photolithography, giving us a possibility of correcting the vertex gap and edge shift in the future, if needed.

4. LABORATORY EXPERIMENT AND RESULTS

4.1. Laboratory experiment setup

In order to first demonstrate the capabilities of the four-quadrant phase mask coronagraph for star light extinction, we have developed a laboratory breadboard. The goal was to be able to test the devices with a setup close to the one envisioned for the on-sky experiment to be conducted at Palomar. The relatively short wavelength range chosen here has allowed the rapid development of a breadboard based on optics used in transmission. An IR single-mode fiber combined with a lens simulates the star. A diaphragm is then used as the entrance pupil, and the collimated beam is focused on the crosshair of the FQPM. The F/# of the beam focused onto the FQPM is the same as for the on-sky experiment. However, with the beam size being set by a diaphragm, the F/# can be varied if one wants to test the influence of this parameter. In the same way, the Lyot stop, used to block the light that is diffracted outside the pupil by the FQPM, has a variable size to find the optimal solution: blocking the maximal amount of the on-axis star light without reducing too much the pupil size to keep a good signal to noise ratio for the companion. The entrance pupil and the Lyot stop are conjugated planes through our optical setup. Different filters can be inserted in the optical beam, allowing testing the performances with varying central wavelength and wavelength range. The FQPM holder allows fine translations to locate it perfectly at the focal point of the optics. A rotation stage allows for fine-tuning of the phase-shift, by increasing the thickness of SiO through which the beam travels. A LN2-cooled IR (InSb) camera combined with an adjustable imaging system allows acquiring both focal plane and pupil plane images. The pupil-imaging mode also allows simultaneous imaging of the pupil and the Lyot stop to check their relative centering.

4.2. Laboratory results

A number of FQPM devices have now been tested on the breadboard, the goal being to accurately tune the manufacturing process to the targeted wavelength range, and to investigate nulling performance in the lab. Extinction ratios, i.e. the ratios of the flux in the central pixel in the Airy pattern without the FQPM to the flux of the central pixel of the image obtained with the FQPM, measured with one of our FQPM devices are presented in Fig. 3. The SiO layer on this device has a thickness of about 1385 nm, corresponding to a first attempt to get the desired π-phase shift, based on refractive index assumption from values for SiO bulk material. First measurements with the FQPM placed perpendicular to the beam (normal use of the device) led to an extinction of the flux by a factor of 20 on the central pixel of the image. Measuring the nulling ratio for three filters with
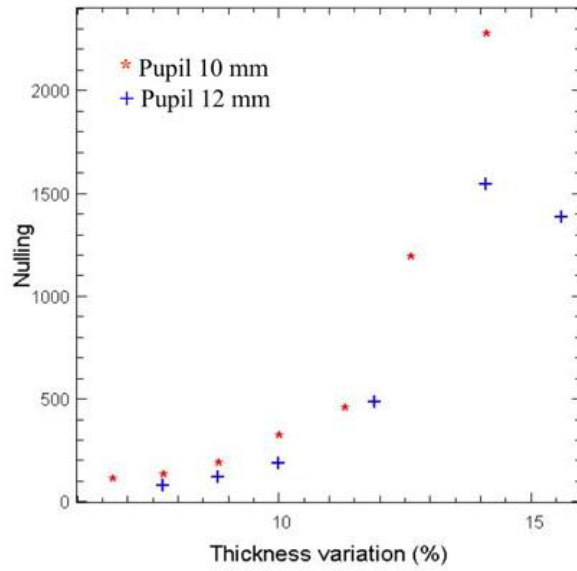
Figure 3. Extinction results with FQPM on the laboratory testbed. Thickness tuning by tilting the device is used to find the best extinction.
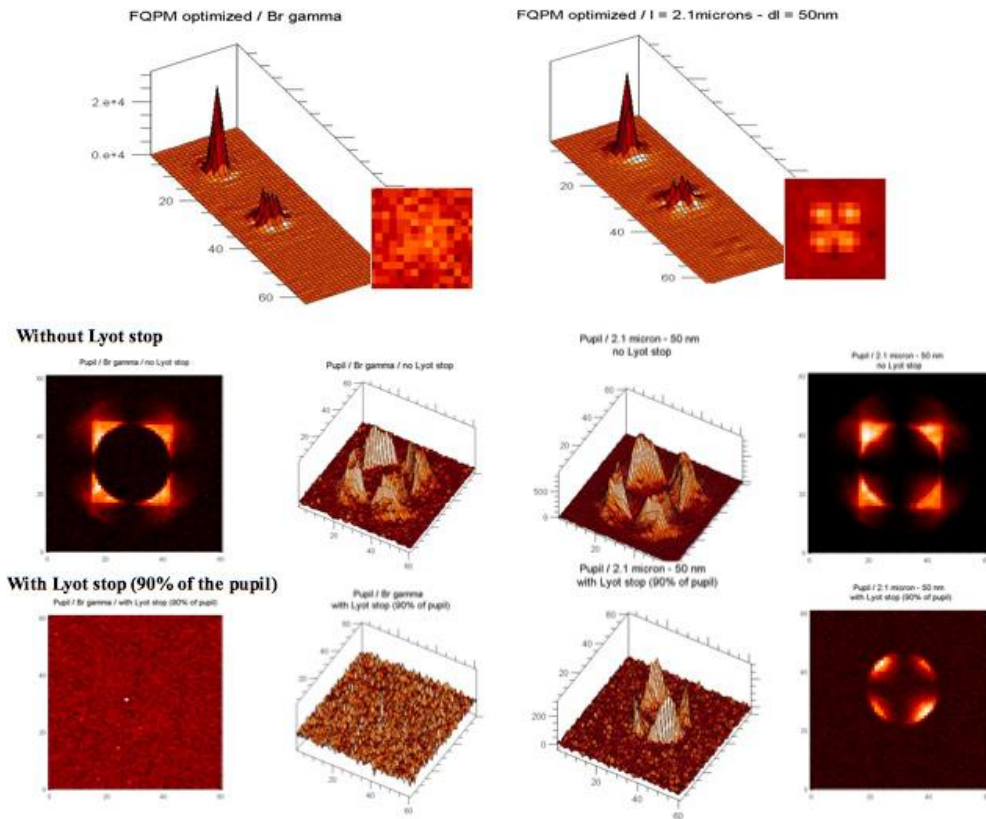
Figure 4. Focal plane (top) and Pupil plane (bottom) images obtained with a FQPM on the laboratory testbed.

different central wavelengths showed increased rejection for the shortest wavelength, clearly indicating that the thickness of the layer was too small. In order to determine the correction factor to apply for the next device, and thus to get an idea of the refractive index difference between bulk material and deposited layer, a rotation stage was added to the FQPM holder, as tilting the device increases the path through the extra dielectric layer. The rotation angle with the best rejection gives the amount by which the thickness has to be increased. The best extinction ratio was 2260:1 on the central pixel of the image (Fig. 3), corresponding to a thickness increase of 14%. The ratio of the brightest pixel of the calibration image to the brightest one on the FQPM image was 500:1 in that case. The tilt angle was optimized for the target wavelength of the Brackett γ filter (central wavelength = $2.168\mu m$). At that point, a filter with a shorter central wavelength did not lead anymore to better nulling results, confirming that the thickness had been optimally tuned. Tilting the device has proven to be a good method for fine-tuning of the FQPM to the wavelength range and to determine the correction to apply to the manufacturing process. New devices have therefore been manufactured, using the new thickness goal derived from the tuning method. Figure 4 top shows images obtained on the camera with the FQPM on and off in different configurations. Two different filters were used here: a Brackett gamma one (left), $\lambda_0 = 2.168\mu m$ and $\Delta\lambda = 19nm$, and one with a wider range (right), $\lambda_0 = 2.1\mu m$ and $\Delta\lambda = 50nm$. On every image, three cases are presented: FQPM out of the beam (used for calibration), FQPM centered on the axis but without the Lyot stop in place, and FQPM with a Lyot stop equal to 90% of the pupil size. The extinction effect of the phase mask is clearly visible here, with almost no light left (at our detection level) in the best case (Brackett gamma with Lyot stop). The capability of imaging the pupil has also been implemented in order to be able to compare the experimental results to the simulations. Images have thus been acquired in different configurations: FQPM tilted or not, with and without the Lyot stop, and for different filters. The obtained images (see Fig. 4) do present the same distributions as the ones predicted by the numerical simulations (see Fig. 1). The effect of a phase-shift not exactly equal to π is to keep more light inside the pupil, as shown by the results with the FQPM perpendicular to the beam or with the FQPM tilted but used with a different central wavelength. With a short passband filter and the FQPM optimized to work at its center wavelength, almost all the light is sent outside of the pupil and a Lyot stop with a size equal to 90% of the pupil diameter allowed removal of this flux (bottom left case). At that level, the remaining flux inside the pupil is barely detectable, the small residual number of photons being confirmed by the 2000:1 rejection level measured on the focal plane images.

5. ON-SKY INSTRUMENT AND MEASUREMENTS

5.1. On-sky instrument design

Four Quadrant Phase Masks can in principle achieve perfect extinction of an on-axis source for a perfectly circular aperture. In the real world, the performances can be highly degraded by beam obstructions like a secondary mirror[12] or spider legs. The perfect light cancellation will also occur only if the incoming wavefront is perfectly plane. Any residual wavefront distortion, coming from both optical elements before the FQPM and atmospheric turbulence, will also lead to a decrease of the maximum achievable extinction. We took these facts into account when designing our ground demonstrator instrument[17]. First, an off-axis configuration of the telescope allows accessing a non-obscured circular pupil. Second, an adaptive optics system (AO) with a high level of correction is required to reduce as much as possible residual wavefront errors. These two points led to the choice of the 5.1m telescope of the Palomar Observatory. The large size of the primary mirror allows using an off-axis part of it with a diameter of still 1.5m, keeping therefore a good angular resolution. The already existing high performance AO on this telescope gives an answer to the second point. Figure 5 presents the setup of the on-sky instrument. Only a few optical elements have to be added to the already existing facilities. A subaperture re-imager allows feeding the AO system with an unobscured pupil, the 1.5m part of the primary being scaled to the full aperture like dimension. One can thus benefit of an AO system designed for a 5.1m telescope on a 1.5m and expect a very high Strehl ratio. To carry out measurements at Palomar, one FQPM has been added in the focal plane of the PHARO[18] camera after the AO system, and an unobscured Lyot stop has also been added.

In order to understand the performance of this approach, we ran numerical simulations of the different cases that can be considered. Figure 6 shows the results of these simulations, with typical turbulence parameters at Mount Palomar and with the specifications of the PALAO system. We first calculate the PSF (through the phase mask) for an on-axis star, and for a star of the same intrinsic brightness at off-axis angle θ_i, and at 45
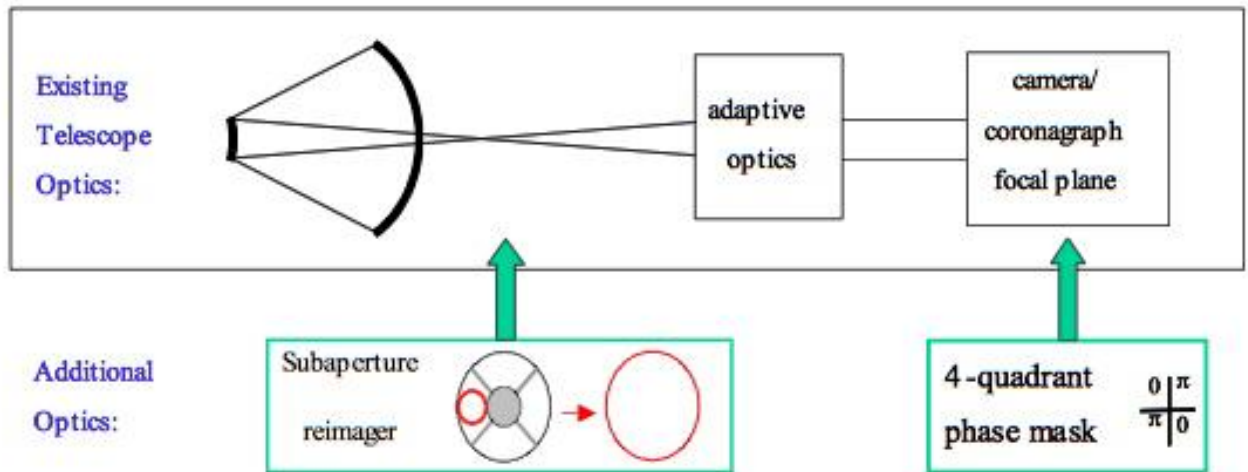
Figure 5. Schematic description of the instrument installed on the Palomar 200 inches telescope.

degrees from the FQPM axis. The plot then shows the ratio of the maximum of the Point Spread Function (PSF) of the companion to the central stars PSF at that angle. The following configurations were tested: both FQPM and classical Lyot coronagraphs for the full 5.1m aperture of the telescope with central obscuration, and both coronagraphs for a 1.5m unobscured off-axis subaperture. The size of the occulting disk for the Lyot cases has been chosen to be four times the diameter of the Airy disk ($4 \times \lambda/D$). On the figure are also represented the diffraction limits (λ/D) of 1.5m and 5.1m telescopes, and the Lyot coronagraph blind zone corresponding to ($4 \times \lambda/D$). Several results are clearly in evidence:

1. With the full aperture telescope including a central obscuration, the FQPM does not give much better performance than the Lyot coronagraph.

2. For an off-axis unobscured subaperture, the gain brought by the FQPM compared to the Lyot case is very significant. Companion detection is possible with very good contrast very close to the diffraction limit of the subaperture. Companion detection is even possible at angular separations below the diffraction limit, as the companion also suffers some extinction but at a lower level than the on-axis star.

3. The subaperture FQPM coronagraph case gives better contrasts in the innermost region (up to about 1.6 arcsec) than any of the other cases, including the full aperture ones. Out to about 1 arc second in radius, and order of magnitude performance improvement is obtained.

5.2. First tests with internal light source

Using the internal white-light source of the PALAO system allowed testing the capabilities of the system on the telescope, before going on-sky. Mechanical arrangement of the camera only allows using the mask perpendicular to the beam (no tilt-tuning), so we are not here at the best working point of this mask. Images with the light focused on the crosshair of the FQPM (on FQPM image), and with light going simply through one quadrant for calibration (off FQPM image), have been taken with the camera in a Brackett gamma filter ($\lambda_0 = 2168nm, \Delta\lambda = 30nm$). A peak extinction (ratio of the flux at the peak of the off FQPM image (r=0) to the flux in the on FQPM image at r=0) of 143:1 was obtained. An extinction ratio on the order of 100:1 on the central pixel was also obtained with a K short filter ($\lambda_0 = 2196nm, \Delta\lambda = 310nm$), in the same conditions.
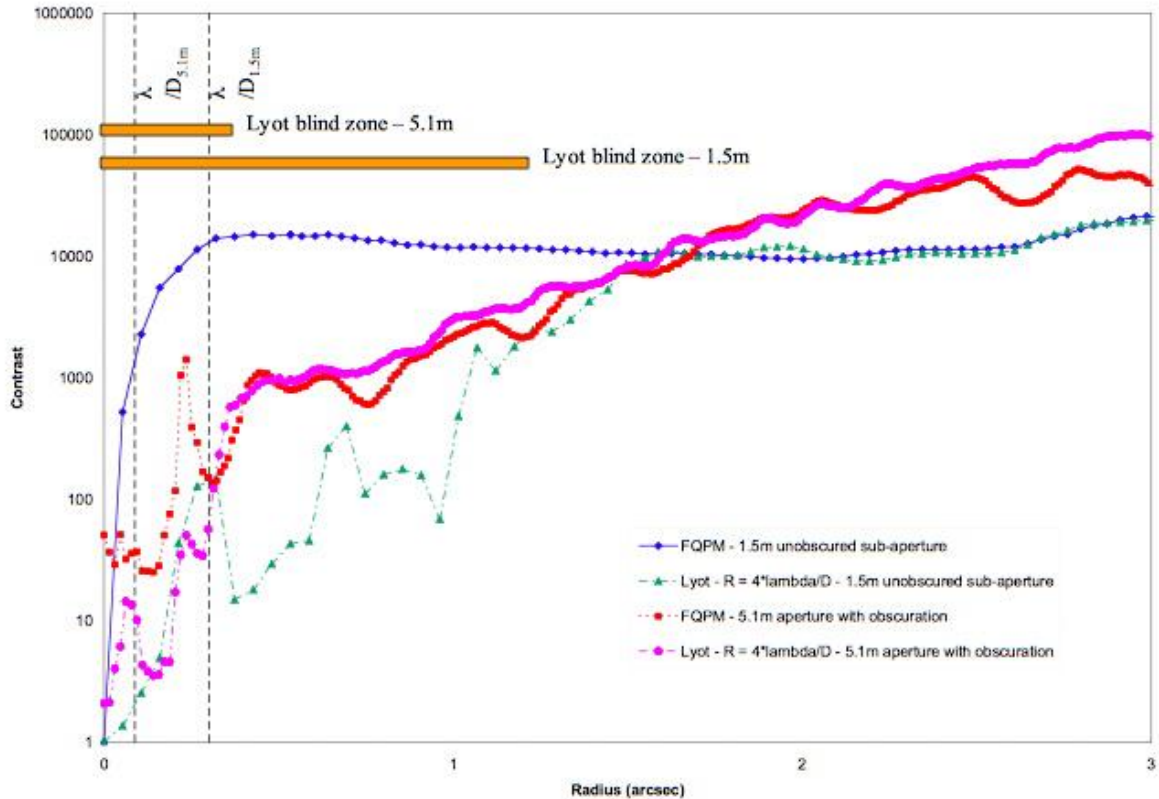
Figure 6. Simulation of performances of FQPM and Lyot coronagraph, in four different configurations of the Palomar 200 inches telescope.

5.3. On-sky results

The first on-sky test of our FQPM instrument was conducted on the 200 inches telescope on Mount Palomar during the nights of June 13th to 15th 2005. Figure 7 and Figure 8 present some of the results obtained during this first observing run. Figure 7 shows FQPM images of a single star, HD121107, in the Brackett γ filter. The left-hand image presents the effect of the phase mask on the flux of the star. The off FQPM corresponds to the image when the light simply goes through one of the quadrants, i.e. without a uniform phase shift across the PSF, and the on FQPM image to the case where the stellar image is centered on the quadrant crosshairs. The same scale has been used here to clearly show the extinction of an on-axis object. The extinction measured here is 110:1, i.e. 5.1 magnitudes (ratio between the brightest pixel of the calibration image and the brightest pixel of the FQPM image). The right-hand images in the figure present the on FQPM 2D and 3D images scaled for better clarity. The residual light image shown has roughly the shape expected from the simulations (see Fig. 1), with a four lobes pattern around the center of the FQPM crosshair. It is however somewhat distorted into a diamond pattern. Figure 8 presents the same results for a binary star, HD148112. The same images are presented here. On the off FQPM image, one can see the companion that lies between the first and second Airy rings of the bright parent star, but its parameters (flux, separation) determination is perturbed by these rings, as they have comparable flux levels. Centering the brighter star on the FQPM then allows a very clear view of its companion (in the off FQPM image) as the flux level of the remaining light from the intrinsically brighter star is now significantly below that of the dimmer companion. The extinction ratio on the parent star was here 74:1, i.e. 4.7 magnitudes, with the Brackett gamma filter. The flux ratio measured here between the two stars is 23:1, and their separation is 0.730 arcsec. The diffraction limit of a 1.5 m aperture is 0.370 arcsec, so this off-axis phase mask coronagraph approach has already successfully allowed imaging of a companion about $2 \times \lambda/D$ away
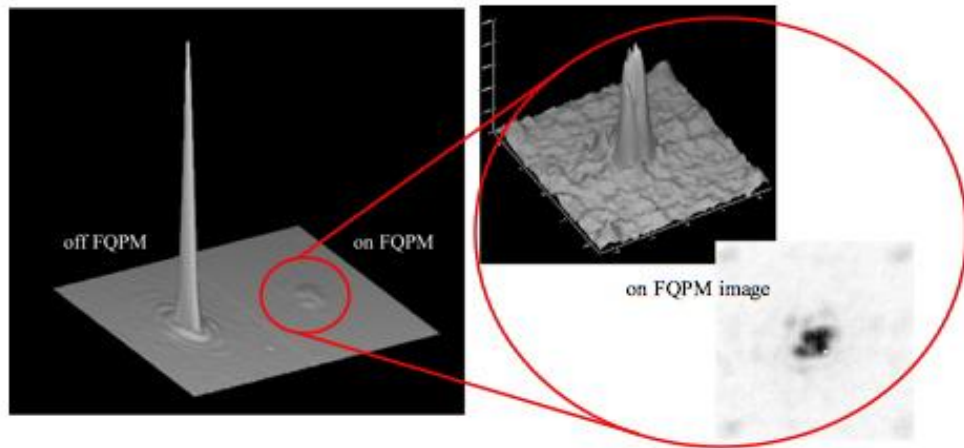
Figure 7. Image of a single star (HD121107) through the FQPM instrument. Left: images obtained with the star centered on the crosshair of the mask (on FQPM), and going through one quadrant for calibration (off FQPM). The extinction ratio obtained here is 110:1. Right: closer view of the on FQPM image.
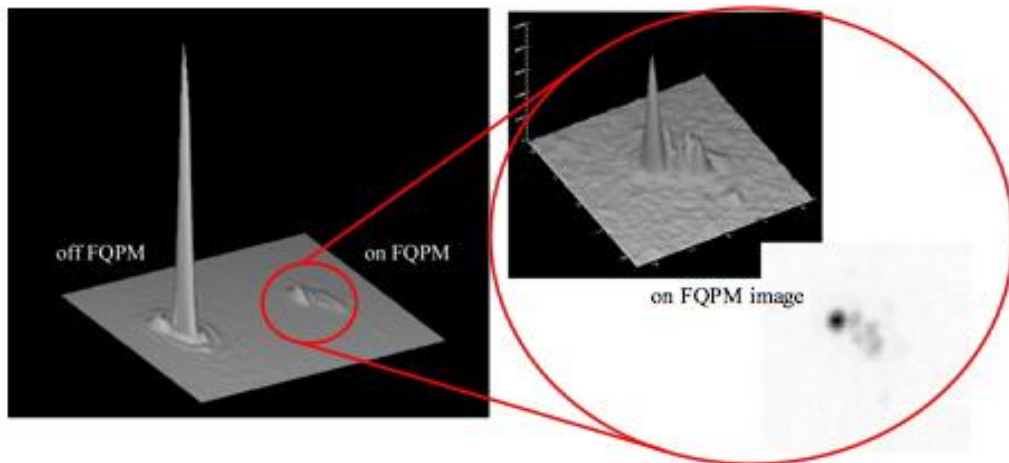
Figure 8. Image of a binary star (HD148112) through the FQPM instrument. Left: images obtained with the star centered on the crosshair of the mask (on FQPM), and going through one quadrant for calibration (off FQPM). Right: closer view of the on FQPM image. The companion is now the brightest peak.

from a star 3.5 mag brighter. As we refine the technique, the results should improve correspondingly.

We have thus validated here our approach of using FQPM with an unobscured pupil and high level AO correction. On-sky results with a FQPM coronagraph have been published elsewhere[14], using there an 8m class telescope but with central obscuration. The peak extinctions were there limited to about 10:1, with the limit imposed mainly by residual wavefront errors not corrected by the AO system.

6. CONCLUSIONS

An innovative off-axis coronagraph concept was developed and taken to the telescope. Our first coronagraphic phase-masks using the four quadrant technique have been successfully manufactured, with laboratory rejections as high as 2260:1. The current design of the masks is optimized for one particular wavelength, but allows for operation in moderately wide wavelength bands with moderate performance. Future efforts will involve increasing the maximum rejection ratio and broadening the band.

Numerical simulations have been conducted in order to take full advantage of this new type of unobscured, off-axis coronagraph, which showed a regime of increased contrast near-bright stars, compared to more classical coronagraph designs. We then designed and successfully installed our coronagraph on the Palomar 200 inches telescope (CA, USA). Our instrument has been designed as an add-on system to the Palomar Adaptive Optics (PALAO) instrument, and takes advantage of the high AO-performance level.

A first on-sky run in June 2005 has proven the very promising capabilities of this combination of off-axis telescope and coronagraphic phase mask. Extinction ratios on stars as high as 110:1 have been obtained in the near-infrared with a passband of 1.3%. Detection capabilities of faint companions in the very close neighborhood of bright stars have also been demonstrated. With the experience acquired with this first on-sky run in terms of operation of this new type of coronagraph, one can now envision increasing the rejection ratio and the wavelength range through mask optimization and new designs.

ACKNOWLEDGMENTS

References

[1] B. Lyot, "The study of the solar corona and prominences without eclipses", MNRAS, Volume 99, p. 580, (1939).

[2] F. Roddier, and C. Roddier, Stellar Coronograph with Phase Mask, The Publications of the Astronomical Society of the Pacific, Volume 109, pp.815-820 (1997).

[3] D. Rouan, P. Riaud, A. Boccaletti, Y. Clenet, and A. Labeyrie, The Four-Quadrant Phase-Mask Coronagraph. I. Principle, The Publications of the Astronomical Society of the Pacific, Volume 112, Issue 777, pp. 1479-1486 (2000).

[4] P. Baudoz, J. Gay, and Y. Rabbia, Achromatic interfero coronagraphy I. Theoretical capabilities for ground-based observations, Astronomy & Astrophysics Supplement, Volume 141, pp.319-329 (2000).

[5] C. Aime, R. Soummer, and A. Ferrari, Interferometric apodization of rectangular apertures. Application to stellar coronagraphy, Astronomy & Astrophysics, Volume 379, pp.697-707 (2001).

[6] D. Spergel, and J. Kasdin, A Shaped Pupil Coronagraph: A Simpler Path towards TPF, 199th American Astronomical Society Meeting, Bulletin of the AAS, Volume 33, p.1431 (2001).

[7] M.J. Kuchner, and W.A. Traub, A Coronagraph with a Band-limited Mask for Finding Terrestrial Planets, The Astrophysical Journal, Volume 570, Issue 2, pp. 900-908 (2002).

[8] O. Guyon, Phase-induced amplitude apodization of telescope pupils for extrasolar terrestrial planet imaging, Astronomy & Astrophysics, Volume 404, pp.379-387 (2003).

[9] R. Soummer, K. Dohlen, and C. Aime, Achromatic dual-zone phase mask stellar coronagraph, Astronomy & Astrophysics, Volume 403, pp.369-381 (2003).

[10] N.J. Kasdin, R.J. Vanderbei, M.G. Littman, and D.N. Spergel, Optimal one-dimensional apodizations and shaped pupils for planet finding coronagraphy, Applied Optics, Volume 44, Issue 7, pp.1117-1128 (2005).

[11] J.P. Lloyd, D.T. Gavel, J.R Graham, P.E. Hodge, A. Sivaramakrishnan, and G.M. Voit, Four-quadrant phase mask coronagraph: analytical calculation and pupil geometry, Proc. SPIE, Volume 4860, pp. 171-181 (2003).

[12] P. Riaud, A. Boccaletti, D. Rouan, F. Lemarquis, and A. Labeyrie, The Four-Quadrant Phase-Mask Coronagraph. II. Simulations, The Publications of the Astronomical Society of the Pacific, Volume 113, Issue 787, pp. 1145-1154 (2001).

[13] P. Riaud, A. Boccaletti, J. Baudrand, and D. Rouan, The Four-Quadrant Phase Mask Coronagraph. III. Laboratory Performance, The Publications of the Astronomical Society of the Pacific, Volume 115, Issue 808, pp. 712-719 (2003).

[14] A. Boccaletti, P. Riaud, P. Baudoz, J. Baudrand, D. Rouan, D. Gratadour, F. Lacombe, and A.-M. Lagrange, The Four-Quadrant Phase Mask Coronagraph. IV. First Light at the Very Large Telescope, The Publications of the Astronomical Society of the Pacific, Volume 116, Issue 825, pp. 1061-1071 (2004).

[15] D. Mawet, C. Lenearts, V. Moreau, Y. L. M. Renotte, D. Rouan, and J. Surdej, Achromatic four quadrants phase mask coronagraph using the dispersion of form birefringence, Proc. SPIE, Volume 4860, pp. 182-191 (2003).

[16] M. Troy, R. Dekany, G. Brack, B. Oppenheimer, E. Bloemhof, T. Trinh, F. Dekens, F. Shi, T. Hayward, and B. Brandl, Palomar adaptive optics project: status and performances, Proc. SPIE, Volume 4007, pp. 31-40 (2000).

[17] G. Serabyn, P. Haguenauer, C. Koresko, An off-axis coronagraph for near neighbor detection, (in preparation).

[18] T.L Hayward, B. Brandl, B. Pirger, C. Blackenm, G.E. Gull, J. Schoenwald, and J.R. Houck, PHARO A Near-Infrared Camera for the Palomar Adaptive Optics System, The Publications of the Astronomical Society of the Pacific, Volume 113, Issue 779, pp. 105-118 (2001).